

## Broad resonance structure in $e^+e^- \rightarrow f_1(1285)\pi^+\pi^-$ and higher $\rho$ -meson excitations

Xiang Liu<sup>1,2,3,4,\*</sup>, Qin-Song Zhou,<sup>1,3,†</sup> and Li-Ming Wang<sup>5,3,‡</sup>

<sup>1</sup>*School of Physical Science and Technology, Lanzhou University, Lanzhou 730000, China*

<sup>2</sup>*Joint Research Center for Physics, Lanzhou University and Qinghai Normal University, Xining 810000, China*

<sup>3</sup>*Lanzhou Center for Theoretical Physics, Key Laboratory of Theoretical Physics of Gansu Province, and Frontiers Science Center for Rare Isotopes, Lanzhou University, Lanzhou 730000, China*

<sup>4</sup>*Research Center for Hadron and CSR Physics, Lanzhou University and Institute of Modern Physics of CAS, Lanzhou 730000, China*

<sup>5</sup>*Key Laboratory for Microstructural Material Physics of Hebei Province, School of Science, Yanshan University, Qinhuangdao 066004, China*



(Received 23 September 2022; accepted 26 October 2022; published 9 November 2022)

Recently, the *BABAR* Collaboration reported a broad resonance structure near 2 GeV when analyzing the  $e^+e^- \rightarrow f_1(1285)\pi^+\pi^-$  process, which provides a good opportunity to study the higher  $\rho$ -mesonic states. When considering the  $\rho(1900)$  and  $\rho(2150)$  contributions, the experimental data of the cross section of  $e^+e^- \rightarrow f_1(1285)\pi^+\pi^-$  around 2 GeV can be well depicted, especially the observed broad resonance structure in  $e^+e^- \rightarrow f_1(1285)\pi^+\pi^-$  containing two substructures is suggested by the present work. Additionally, we also indicate a possible signal of  $\rho(5S)$  around 2.5 GeV in the  $e^+e^- \rightarrow f_1(1285)\pi^+\pi^-$  process. The obtained result may provide a valuable hint to identify higher  $\rho$  mesons, which will be a new task for the BESIII and Belle II experiments with the accumulation of higher precision data.

DOI: [10.1103/PhysRevD.106.094012](https://doi.org/10.1103/PhysRevD.106.094012)

### I. INTRODUCTION

Very recently, the *BABAR* Collaboration announced the measurement of the  $e^+e^- \rightarrow K^+K^-3\pi^0$ ,  $e^+e^- \rightarrow K_S^0K^\pm\pi^\mp 2\pi^0$ , and  $e^+e^- \rightarrow K_S^0K^\pm\pi^\mp\pi^+\pi^-$  processes at center-of-mass energies from threshold to 4.5 GeV, where this analysis was performed with the initial state radiation method [1]. By the  $e^+e^- \rightarrow K_S^0K^\pm\pi^\mp\pi^+\pi^-$  reaction, *BABAR* reconstructed the  $e^+e^- \rightarrow f_1(1285)\pi^+\pi^-$  process, by which a broad enhancement structure around 2 GeV was observed with resonance parameters

$$M = 2.09 \pm 0.03 \text{ GeV}, \quad \Gamma = 0.50 \pm 0.06 \text{ GeV}.$$

Actually, in 2007, the *BABAR* Collaboration had already studied the  $e^+e^- \rightarrow f_1(1285)\pi^+\pi^-$  process [2], and a broad resonance structure was observed around 2 GeV by a single Breit-Wigner fitting, which has resonance parameters

$$M = 2.15 \pm 0.04 \pm 0.05 \text{ GeV},$$

$$\Gamma = 0.35 \pm 0.04 \pm 0.05 \text{ GeV}.$$

Here, the experimental results for the cross section of  $e^+e^- \rightarrow f_1(1285)\pi^+\pi^-$  are collected in Fig. 1. Because of the constraint of conservations of angular momentum and  $P$  parity, it requires that the  $f_1(1285)\pi^+\pi^-$  system must have a quantum number  $I^G(J^{PC}) = 1^+(1^{--})$ . Therefore, the measured  $e^+e^- \rightarrow f_1(1285)\pi^+\pi^-$  process may provide a good chance to construct the  $\rho$ -meson family.

In the mass region around 2 GeV, there are three  $\rho$ -mesonic states collected in the Particle Data Group (PDG) [3], which are the  $\rho(1900)$ ,  $\rho(2150)$ , and  $\rho(2000)$ . Although experiments have reported some  $\rho$  states around 2 GeV in the past few decades [3], categorizing these states into the  $\rho$ -meson family is far from being established. In Fig. 2, we list the resonance parameters of the  $\rho(1900)$  and  $\rho(2150)$  measured by different experiment groups [3], by which the messy situation of the measured resonance parameters of these two higher  $\rho$  states around 2 GeV is presented. Evidently, the resonance parameters of the  $\rho(1900)$  and  $\rho(2150)$  from different experiments are different. If considering the experimental uncertainties, the obtained widths of the  $\rho(1900)$  and  $\rho(2150)$  are in the ranges of 5–180 and 32–630 MeV, respectively. The  $\rho(2000)$  is collected in PDG as the “further state” [3],

\*xiangliu@lzu.edu.cn

†zhouqs13@lzu.edu.cn

‡lmwang@ysu.edu.cn

Published by the American Physical Society under the terms of the [Creative Commons Attribution 4.0 International license](https://creativecommons.org/licenses/by/4.0/). Further distribution of this work must maintain attribution to the author(s) and the published article’s title, journal citation, and DOI. Funded by SCOAP<sup>3</sup>.

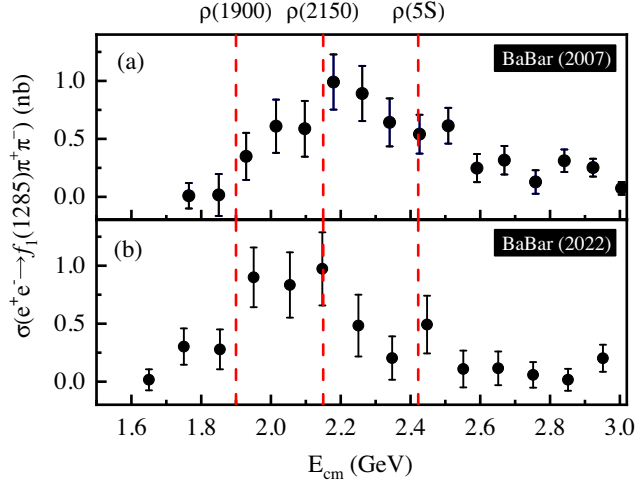


FIG. 1. The experimental data of  $e^+e^- \rightarrow f_1(1285)\pi^+\pi^-$ . Here, the experimental data shown in (a) were measured by the *BABAR* Collaboration in 2007 [2], and the result in (b) was newly measured by the *BABAR* Collaboration in 2022 [1].

which was first reported by an amplitude analysis of the data of  $p\bar{p} \rightarrow \pi\pi$  [4]. After that, its existence was confirmed by a combined analysis of the  $e^+e^- \rightarrow \omega\eta\pi^0$  and  $\omega\pi$  [5]. However, many recent experimental measurements with higher precision for the  $\rho$ -mesonic states show that there is an enhancement structure with the width around 100 MeV and the mass near 2 GeV rather than a broad structure with the width larger than 300 MeV [6,7]. On the theoretical side, various models have also been used to study the mass spectrum of  $\rho$  mesons, including potential model [8–13], Regge trajectory [14,15], and other methods [16–18], where the  $\rho(1900)$ ,  $\rho(2150)$ , and  $\rho(2000)$  are usually categorized as  $\rho(3^3S_1) \equiv \rho(3S)$ ,  $\rho(4^3S_1) \equiv \rho(4S)$ , and  $\rho(2^3D_1) \equiv \rho(2D)$ , respectively. The quark pair creation (QPC) model is widely applied to estimate Okubo-Zweig-lizuka (OZI)-allowed two-body strong decays of a hadron. By using the QPC model [11–15], the widths of

higher  $\rho$  mesons were obtained, where the calculated widths of the  $\rho(1900)$ ,  $\rho(2105)$ , and  $\rho(2000)$  are in the ranges of 125–184, 102–122, and 179–228 MeV, respectively.

As mentioned above, we briefly review the status of experimental and theoretical research on  $\rho$ -mesonic states around 2 GeV. When facing *BABAR*'s measurement of the cross section of the  $e^+e^- \rightarrow f_1(1285)\pi^+\pi^-$  process, some questions are raised as shown below. Usually, the theoretical results show that the widths of the  $\rho(1900)$  and  $\rho(2150)$  are about 100 MeV, and the width of the  $\rho(2000)$  is less than 300 MeV. Obviously, the broad structure observed by the *BABAR* Collaboration in the  $e^+e^- \rightarrow f_1(1285)\pi^+\pi^-$  process is not consistent with these reported  $\rho$  states. Can we find a solution to alleviate such inconsistency?

To clarify this issue, we conjecture that the reported broad structure in the  $f_1(1285)\pi^+\pi^-$  invariant mass spectrum can be still due to the interference effect from some higher  $\rho$ -mesonic states. According to the theoretical study of higher  $\rho$ -mesonic states around and above 2 GeV by the modified Godfrey-Isgur model [11–13], we suggest that the  $\rho(3S)$ ,  $\rho(4S)$ , and  $\rho(5S)$  contribution should be introduced when depicting the data of the  $e^+e^- \rightarrow f_1(1285)\pi^+\pi^-$  process, where the  $\rho(3S)$  and  $\rho(4S)$  correspond to the  $\rho(1900)$  and  $\rho(2150)$ , respectively. In realistic calculation, we adopt the effective Lagrangian approach to calculate the cross section of  $e^+e^- \rightarrow \rho^* \rightarrow f_1(1285)\pi^+\pi^-$ . By fitting the experimental data of the cross section of  $e^+e^- \rightarrow f_1(1285)\pi^+\pi^-$ , we find that the reported broad enhancement structure in  $e^+e^- \rightarrow f_1(1285)\pi^+\pi^-$  may contain two substructures, i.e., the  $\rho(1900)$  and  $\rho(2150)$ . In addition, we also find possible evidence of  $\rho(5S)$  when reproducing the line shape of the cross section of  $e^+e^- \rightarrow f_1(1285)\pi^+\pi^-$  well. With more precise data collected by BESIII and Belle II in the near future, we have reason to believe that our observations can be tested.

This paper is organized as follows. After the introduction, we illustrate the study of the  $e^+e^- \rightarrow f_1(1285)\pi^+\pi^-$

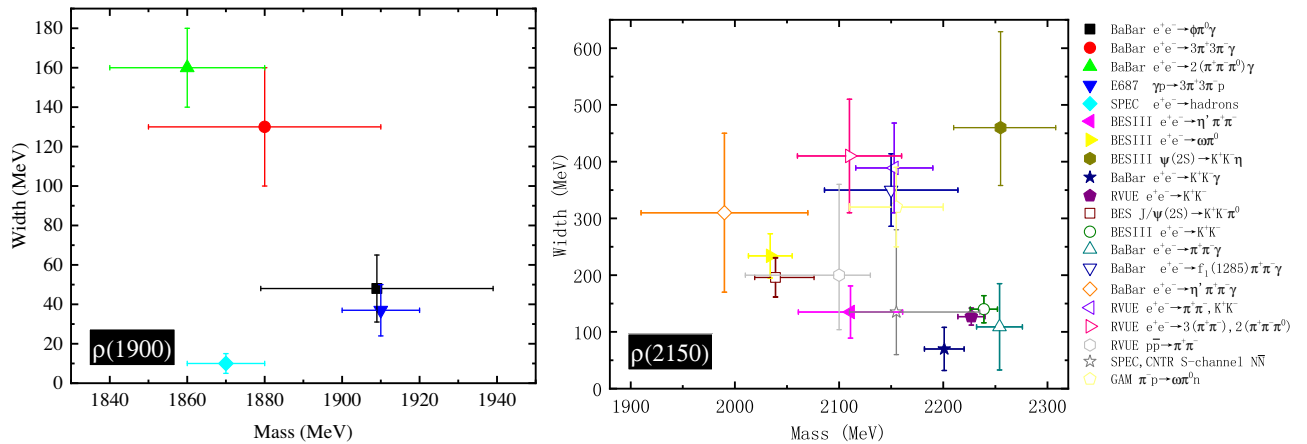


FIG. 2. The resonance parameters of the  $\rho(1900)$  and  $\rho(2150)$  are measured by different experiments collected in PDG [3].

process by considering the intermediate higher  $\rho$  mesons as shown in Sec. II. In Sec. III, we present numerical results for the analysis of the cross section of the  $e^+e^- \rightarrow f_1(1285)\pi^+\pi^-$  process. Finally, the paper ends with a discussion and conclusion in Sec. IV.

## II. HIGHER $\rho$ -MESONIC STATE CONTRIBUTIONS TO $e^+e^- \rightarrow f_1(1285)\pi^+\pi^-$

Since the scatter plot of  $m(\pi^+\pi^-)$  vs  $m(K_S^0 K^\pm \pi^\pm)$  given by the *BABAR* Collaboration [1] shows that  $\pi^+\pi^-$  is dominantly from  $\rho(770)$ , we can assume that the reaction  $e^+e^- \rightarrow f_1(1285)\pi^+\pi^-$  occurs mainly through the two reaction mechanisms shown in Fig. 3. Here, Fig. 3(a) depicts the virtual photon directly coupled with  $f_1(1285)\rho$ , which provides the background contribution, while Fig. 3(b) reflects intermediate higher  $\rho$ -meson contribution to  $e^+e^- \rightarrow f_1(1285)\pi^+\pi^-$ .

In this work, we adopt the effective Lagrangian approach to describe these interaction vertices shown in Fig. 3. The effective Lagrangians involved in the concrete calculation include [19–23]

$$\mathcal{L}_{\gamma f_1 \rho} = g_{\gamma f_1 \rho} \epsilon^{\mu\nu\alpha\beta} (\partial_\mu A_\alpha \partial^\lambda \partial_\lambda \rho_\nu - \partial^\lambda \partial_\lambda A_\alpha \partial_\mu \rho_\nu) f_{1\beta}, \quad (1)$$

$$\mathcal{L}_{\rho^* f_1 \rho} = g_{\rho^* f_1 \rho} \epsilon^{\mu\nu\alpha\beta} (\partial_\mu \rho_\alpha^* \partial^\lambda \partial_\lambda \rho_\nu - \partial^\lambda \partial_\lambda \rho_\alpha^* \partial_\mu \rho_\nu) f_{1\beta}, \quad (2)$$

$$\mathcal{L}_{\rho\pi\pi} = g_{\rho\pi\pi} \rho^\mu \overleftrightarrow{\partial}_\mu \pi, \quad (3)$$

$$\mathcal{L}_{\gamma\rho^*} = -e \frac{m_{\rho^*}^2}{f_{\rho^*}} \rho^{*\mu} A_\mu, \quad (4)$$

where  $\rho^*$ ,  $\rho$ ,  $f_1$ , and  $\pi$  stand for the mesonic fields of higher  $\rho$  meson,  $\rho(770)$ ,  $f_1(1285)$ , and  $\pi$ , respectively. With the above preparation, the amplitude of  $e^+e^- \rightarrow f_1(1285)\pi^+\pi^-$  corresponding to Fig. 3(a) is written as

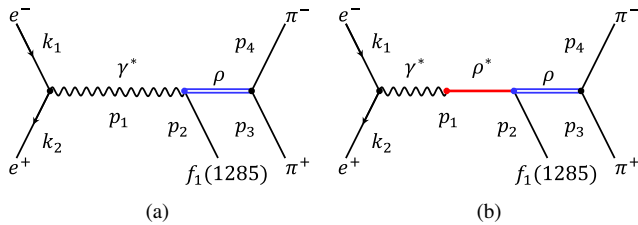


FIG. 3. The schematic diagrams depict the reaction  $e^+e^- \rightarrow f_1(1285)\pi^+\pi^-$ . Here, (a) depicts the virtual photon directly coupling to  $f_1(1285)\rho$ , while (b) is due to the intermediate state  $\rho^*$  contribution, where  $\rho^*$  denotes higher  $\rho$ -mesonic states.

$$\begin{aligned} \mathcal{M}_{\text{Dir}} &= g_{\gamma^* f_1 \rho} g_{\rho\pi\pi} \bar{v}(k_2) (ie\gamma_\sigma) u(k_1) \\ &\times \frac{-g^{\sigma\alpha}}{p_1^2} \epsilon^{\mu\nu\alpha\beta} (p_{1\mu} q^2 + p_1^2 q_\mu) \\ &\times \frac{\tilde{g}_{\nu\kappa}(q)}{q^2 - m_\rho^2 + im_\rho \Gamma_\rho} (p_4^\kappa - p_3^\kappa) \epsilon^{*\beta}(p_2) \mathcal{F}(s), \end{aligned} \quad (5)$$

where  $p_2$ ,  $p_3$ , and  $p_4$  are the four momenta of final states  $f_1(1285)$ ,  $\pi^+$ , and  $\pi^-$ , respectively. And,  $p_1 = k_1 + k_2$ ,  $q = p_3 + p_4$ ,  $\tilde{g}^{\nu\kappa}(q) = -g^{\nu\kappa} + q^\nu q^\kappa / q^2$ , and the form factor  $\mathcal{F}(s) = e^{-b[\sqrt{s} - (m_{f_1(1285)} + m_{\pi^+} + m_{\pi^-})]}$  are defined. The amplitude of the reaction of  $e^+e^- \rightarrow f_1(1285)\pi^+\pi^-$  via the intermediate higher  $\rho$  state, which corresponds to Fig. 3(b), can be written as the product of the amplitude of  $e^+e^- \rightarrow \rho_i^*$  and the amplitude of  $\rho_i^* \rightarrow f_1(1285)\pi^+\pi^-$ :

$$\mathcal{M}_{\rho_i^*} = \frac{\mathcal{M}_{e^+e^- \rightarrow \rho_i^*} \mathcal{M}_{\rho_i^* \rightarrow f_1(1285)\pi^+\pi^-}}{p_1^2 - m_{\rho_i^*}^2 + im_{\rho_i^*} \Gamma_{\rho_i^*}}, \quad (6)$$

where the amplitude of  $e^+e^- \rightarrow \rho_i^*$  is written as

$$\mathcal{M}_{e^+e^- \rightarrow \rho_i^*} = \bar{v}(k_2) (ie\gamma_\sigma) u(k_1) \frac{-g^{\sigma\alpha} - em_{\rho_i^*}^2}{p_1^2} \frac{1}{f_{\rho_i^*}} \epsilon^{*\alpha}(p_1) \quad (7)$$

and the amplitude of  $\rho_i^* \rightarrow f_1(1285)\pi^+\pi^-$  is expressed as

$$\begin{aligned} \mathcal{M}_{\rho_i^* \rightarrow f_1(1285)\pi^+\pi^-} &= g_{\rho_i^* f_1(1285)\rho} g_{\rho\pi\pi} \\ &\times \epsilon^\alpha(p_1) \epsilon^{\mu\nu\alpha\beta} (p_{1\mu} q^2 + p_1^2 q_\mu) \\ &\times \frac{\tilde{g}_{\nu\kappa}(q)}{q^2 - m_\rho^2 + im_\rho \Gamma_\rho} (p_4^\kappa - p_3^\kappa) \epsilon^{*\beta}(p_2). \end{aligned} \quad (8)$$

With the partial decay width of  $\rho(770) \rightarrow \pi\pi$  listed in PDG [3], we estimate the coupling constant  $g_{\rho\pi\pi} = 6 \text{ GeV}^{-2}$ .

The differential cross section of  $e^+e^- \rightarrow f_1(1285)\pi^+\pi^-$  is

$$d\sigma = \frac{1}{32(2\pi)^5 \sqrt{s} \sqrt{k_1 k_2}} |\overline{\mathcal{M}_{\text{Total}}}|^2 |\vec{p}_2| |\vec{p}_3| d\Omega_2 d\Omega_3^* dm_{34}, \quad (9)$$

where  $\vec{p}_2$  ( $\Omega_2$ ) is the three-momentum (solid angle) of  $f_1(1285)$  in the center-of-mass frame,  $\vec{p}_3^*$  ( $\Omega_3^*$ ) stands for the three-momentum (solid angle) of the  $\pi^+$  in the rest frame of  $\pi^+$  and  $\pi^-$ , and  $m_{34}$  is the invariant mass of the  $\pi^+$  and  $\pi^-$  system. On the other hand, the total amplitude of  $\mathcal{M}_{\text{Total}}$  is

$$\mathcal{M}_{\text{Total}} = \mathcal{M}_{\text{Dir}} + \sum_{\rho_i^*} \mathcal{M}_{\rho_i^*} e^{i\phi_{\rho_i^*}}. \quad (10)$$

Here,  $\rho_i^*$  denote the allowed higher  $\rho$ -meson states, while  $\phi_{\rho_i^*}$  is the phase angle among different amplitudes, which is determined by fitting experimental data. In addition, these

coupling constants included in the amplitudes are also determined by fitting experimental data.

To facilitate comparison with the experimental results, the combined branching ratio  $\Gamma_{e^+e^-}\mathcal{B}(\rho_i^* \rightarrow f_1(1285)\pi^+\pi^-)$  can be calculated by using Eqs. (11) and (12) when the coupling constants are obtained by fitting the experimental data, where  $\Gamma_{e^+e^-}$  is the dilepton decay width of  $\rho_i^*$ , i.e.,

$$\Gamma_{e^+e^-} = \frac{e^4 m_{\rho_i^*}}{12\pi f_{\rho_i^*}^2}. \quad (11)$$

Then, the  $\mathcal{B}(\rho_i^* \rightarrow f_1(1285)\pi^+\pi^-) = \Gamma(\rho_i^* \rightarrow f_1(1285)\pi^+\pi^-)/\Gamma_{\rho_i^*}$  denotes the branching ratio of  $\rho_i^* \rightarrow f_1(1285)\pi^+\pi^-$  with the expression

$$\begin{aligned} \Gamma(\rho_i^* \rightarrow f_1(1285)\pi^+\pi^-) &= \frac{1}{(2\pi)^5} \frac{1}{16m_{\rho_i^*}^2} |\mathcal{M}_{\rho_i^* \rightarrow f_1(1285)\pi^+\pi^-}|^2 \\ &\times |\vec{p}_2| |\vec{p}_3| d\Omega_2 d\Omega_3^* dm_{34}. \end{aligned} \quad (12)$$

Here, all symbols have the same meaning as in Eq. (9).

### III. NUMERICAL RESULTS

In this section, we adopt two schemes to fit the experimental data of the cross section of  $e^+e^- \rightarrow f_1(1285)\pi^+\pi^-$  measured by the *BABAR* Collaboration [1,2]. In scheme 1, we consider the contributions of these higher  $\rho$ -mesonic states near 2 GeV, which include the  $\rho(1900)$ ,  $\rho(2150)$ , and  $\rho(2000)$ , to decipher the broad resonance structure existing in the  $e^+e^- \rightarrow f_1(1285)\pi^+\pi^-$  process. We also notice that there is an event accumulation around 2.5 GeV. Thus, in scheme 2,  $\rho(5S)$  associated with the  $\rho(1900)$ ,  $\rho(2150)$ , and  $\rho(2000)$  is considered for depicting the data well. In our investigation, these coupling constants, relative phase angles, the resonance parameters of relevant higher  $\rho$ -mesonic states, and the parameter  $b$  in form factor are treated as the fitting parameters.

Although there are three reported  $\rho$  states near 2 GeV, the  $\rho(2000)$  as a typical D-wave state [11,12,14,18] is not included in our study. The main reason is that the dilepton width of the D-wave vector meson is suppressed compared to the case of the S-wave vector meson [8,12,24,25]. Thus, in scheme 1, we consider only the contributions from the  $\rho(1900)$  and  $\rho(2150)$  to reproduce the cross section data of  $e^+e^- \rightarrow f_1(1285)\pi^+\pi^-$  process. The fitted result of the cross sections of  $e^+e^- \rightarrow f_1(1285)\pi^+\pi^-$  is shown in Fig. 4, where these obtained fitting parameters are collected into Table I. For convenience,  $g_{\rho_i^* f_1(1285)\rho} g_{\rho\pi\pi} / f_{\rho_i^*}$  is abbreviated to be  $g_{\rho_i^*}$ . With the central values of the fitted parameters, the value of  $\chi^2/\text{n.d.f.}$  is obtained to be 1.63.

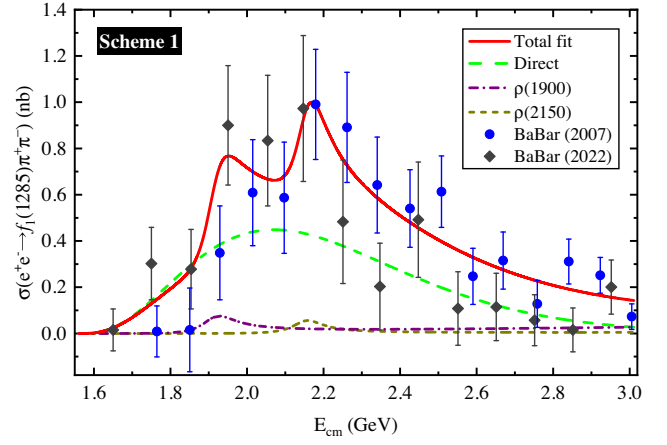


FIG. 4. The fit to the experimental data of the cross sections of  $e^+e^- \rightarrow f_1(1285)\pi^+\pi^-$  measured by the *BABAR* Collaboration in 2007 [2] (blue dots with error bars) and in 2022 [1] (black dots with error bars). In this scheme, only the contributions from the  $\rho(1900)$  and  $\rho(2150)$  are considered. Here, the calculated value of  $\chi^2/\text{n.d.f.}$  is 1.63.

As shown in Fig. 4, the fitted curve can well reproduce the experimental data of the cross sections for  $e^+e^- \rightarrow f_1(1285)\pi^+\pi^-$ . Especially, our study shows that the reported broad enhancement structure in  $e^+e^- \rightarrow f_1(1285)\pi^+\pi^-$  should at least contain two substructures like the  $\rho(1900)$  and  $\rho(2150)$ . We also list the fitted results of the resonance parameters for both  $\rho(1900)$  and  $\rho(2150)$  in Table I, which are within the range of previous theoretical results [10–12,14,15].

By such an effort, we provide a possible explanation to understand why there exists the broad structure with width around 300 MeV in  $e^+e^- \rightarrow f_1(1285)\pi^+\pi^-$ , which is caused by the interference effect of the  $\rho(1900)$  and  $\rho(2150)$ . Thus, the inconsistency of the *BABAR*

TABLE I. The parameters involved in scheme 1, which are obtained by fitting the cross sections of the  $e^+e^- \rightarrow f_1(1285)\pi^+\pi^-$  process. Here, the experimental data are from *BABAR* [1,2].

Parameters	Values
$m_{\rho(1900)}$ (MeV)	$1913 \pm 34$
$m_{\rho(2150)}$ (MeV)	$2151 \pm 32$
$\Gamma_{\rho(1900)}$ (MeV)	$106 \pm 21$
$\Gamma_{\rho(2150)}$ (MeV)	$98 \pm 16$
$g_{\gamma^* \rho f_1(1285)}$ ( $\text{GeV}^{-2}$ )	$4.11 \pm 0.38$
$g_{\rho(1900)}$ ( $\text{GeV}^{-2}$ )	$0.088 \pm 0.009$
$g_{\rho(2150)}$ ( $\text{GeV}^{-2}$ )	$0.024 \pm 0.007$
$b$ ( $\text{GeV}^{-1}$ )	$3.74 \pm 0.18$
$\phi_{\rho(1900)}$ (rad)	$0.63 \pm 0.02$
$\phi_{\rho(2150)}$ (rad)	$0.90 \pm 0.04$
$\chi^2/\text{n.d.f.}$	1.63

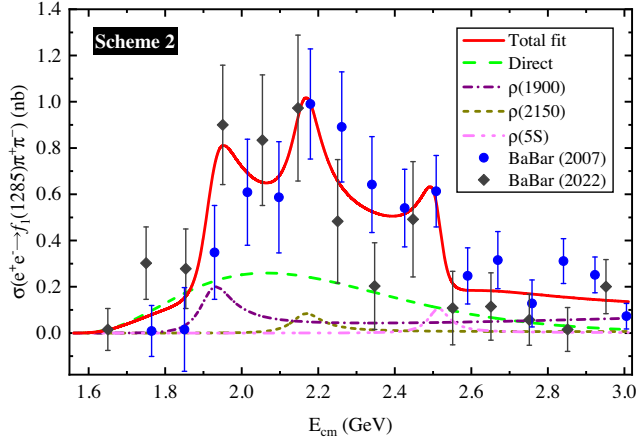


FIG. 5. The fit to the experimental data of the cross sections of  $e^+e^- \rightarrow f_1(1285)\pi^+\pi^-$  measured by the *BABAR* Collaboration in 2007 [2] (blue dots with error bars) and 2022 [1] (black dots with error bars). In this scheme, the contributions from  $\rho(1900)$ ,  $\rho(2150)$ , and  $\rho(5S)$  are considered. Here, the calculated value of  $\chi^2/\text{n.d.f.}$  is 1.52.

observation of very broad enhancement structure [1,2] and the established  $\rho$  states near 2 GeV in PDG can be naturally alleviated.

Besides explaining the broad structure reported by *BABAR*, we notice an event cluster around 2.5 GeV in the measured cross section data. Thus, we propose to include the predicted  $\rho(5S)$  state [11–13] associated with the  $\rho(1900)$  and  $\rho(2150)$ , which is as scheme 2 in the present work. The fitted results are shown in Fig. 5, and the corresponding parameters are listed in Table II. Obviously, the fitting result to the cross section of  $e^+e^- \rightarrow f_1(1285)\pi^+\pi^-$  can be improved in scheme 2. We obtain the resonance parameter of the  $\rho(5S)$  state, i.e.,

TABLE II. The parameters for scheme 2 when fitting the cross sections of the  $e^+e^- \rightarrow f_1(1285)\pi^+\pi^-$  process [1,2].

Parameters	Values
$m_{\rho(1900)}$ (MeV)	$1919 \pm 38$
$m_{\rho(2150)}$ (MeV)	$2162 \pm 31$
$m_{\rho(5S)}$ (MeV)	$2512 \pm 56$
$\Gamma_{\rho(1900)}$ (MeV)	$102 \pm 41$
$\Gamma_{\rho(2150)}$ (MeV)	$95 \pm 28$
$\Gamma_{\rho(5S)}$ (MeV)	$66 \pm 38$
$g_{\gamma^* \rho f_1(1285)}$ ( $\text{GeV}^{-2}$ )	$3.19 \pm 0.10$
$g_{\rho(1900)}$ ( $\text{GeV}^{-2}$ )	$0.133 \pm 0.019$
$g_{\rho(2150)}$ ( $\text{GeV}^{-2}$ )	$0.028 \pm 0.008$
$g_{\rho(5S)}$ ( $\text{GeV}^{-2}$ )	$0.007 \pm 0.002$
$b$ ( $\text{GeV}^{-1}$ )	$3.78 \pm 0.49$
$\phi_{\rho(1900)}$ (rad)	$0.52 \pm 0.21$
$\phi_{\rho(2150)}$ (rad)	$1.47 \pm 0.19$
$\phi_{\rho(5S)}$ (rad)	$3.20 \pm 0.36$
$\chi^2/\text{n.d.f.}$	1.52

TABLE III. The combined branching ratios  $\Gamma_{e^+e^- \mathcal{B}(\rho_i^* \rightarrow f_1(1285)\pi^+\pi^-)}$  are estimated by substituting the values of the coupling constants listed in Table II into Eqs. (11) and (12).

Parameters	Values (eV)
$\Gamma_{e^+e^- \mathcal{B}(\rho(1900) \rightarrow f_1(1285)\pi^+\pi^-)}$	2.08–3.69
$\Gamma_{e^+e^- \mathcal{B}(\rho(2150) \rightarrow f_1(1285)\pi^+\pi^-)}$	5.71–18.48
$\Gamma_{e^+e^- \mathcal{B}(\rho(5^3S_1) \rightarrow f_1(1285)\pi^+\pi^-)}$	0.46–13.04

$$M = 2512 \pm 56 \text{ MeV}, \quad \Gamma = 66 \pm 38 \text{ MeV},$$

which is consistent with theoretical predictions in Refs. [11–13]. We suggest a future experiment to identify the  $\rho(5S)$  signal with more precise data, which is crucial to construct the  $\rho$ -meson family.

To facilitate comparison with the experimental results, by substituting the values of the coupling constants listed in Table II into Eqs. (11) and (12), we can estimate the values of the combined branching ratio  $\Gamma_{e^+e^- \mathcal{B}(\rho_i^* \rightarrow f_1(1285)\pi^+\pi^-)}$ , which are presented in Table III. The values of these combined branching ratios can be measured by experiments with higher precision in the future, by which our scenario proposed in this work can be tested.

#### IV. DISCUSSION AND CONCLUSION

Very recently, the *BABAR* Collaboration measured  $e^+e^- \rightarrow f_1(128)\pi^+\pi^-$  again [1] and reported a very broad enhancement structure around 2 GeV in the  $f_1(128)\pi^+\pi^-$  invariant mass spectrum. In 2007, *BABAR* once indicated a similar phenomenon [2]. If making a comparison of *BABAR*'s observation with these reported  $\rho$  states around 2 GeV collected by PDG [3], the broad enhancement structure from *BABAR* cannot correspond to these reported  $\rho$  states like  $\rho(1900)$ ,  $\rho(2000)$ , and  $\rho(2150)$ . This puzzling phenomenon stimulates our interest.

Supported by the  $\rho$ -meson spectroscopy [11,12,14,18], we propose an interference picture of the  $\rho(1900)$  and  $\rho(2150)$  to depict the observed broad enhancement structure around 2 GeV in the  $e^+e^- \rightarrow f_1(128)\pi^+\pi^-$ . By this approach, the data of the cross section of  $e^+e^- \rightarrow f_1(128)\pi^+\pi^-$  can be reproduced well. Naturally, we provide a natural solution to understand the puzzling phenomenon mentioned above.

In fact, an event cluster around 2.5 GeV can be found if checking the experimental data of the cross section of  $e^+e^- \rightarrow f_1(128)\pi^+\pi^-$ . We notice that different theoretical groups predicted the existence of the  $\rho(5S)$  state. Thus, we include the contribution of the  $\rho(5S)$  state to fit the experimental data again, where the resonance parameter of the  $\rho(5S)$  state can be obtained, which is consistent with the theoretical predictions [11–13]. Confirming this

evidence is a potential issue for our experimental colleagues.

In summary,  $e^+e^- \rightarrow f_1(128)\pi^+\pi^-$  is an ideal process to identify higher  $\rho$ -mesonic states. At present, the  $\rho$ -meson family is far from being established. As one part of the whole hadronic zoo, we have enough interest in finding out new higher  $\rho$ -meson states. With the running of Belle II and BESIII, experimentalists do not stop observing new  $\rho$  states. We hope that the present work may inspire some insights to construct the light flavor vector meson family.

## ACKNOWLEDGMENTS

This work is supported by the projects funded by Science and Technology Department of Qinghai Province (No. 2020-ZJ-728), the China National Funds for Distinguished Young Scientists under Grant No. 11825503, National Key Research and Development Program of China under Contract No. 2020YFA0406400, the 111 Project under Grant No. B20063, and the National Natural Science Foundation of China under Grant No. 12047501.

- 
- [1] J. P. Lees *et al.* (BABAR Collaboration), Study of the reactions  $e^+e^- \rightarrow K^+K^-\pi^0\pi^0\pi^0$ ,  $e^+e^- \rightarrow K_S^0K^\pm\pi^\mp\pi^0\pi^0$ , and  $e^+e^- \rightarrow K_S^0K^\pm\pi^\mp\pi^+\pi^-$  at center-of-mass energies from threshold to 4.5 GeV using ISR, [arXiv:2207.10340](https://arxiv.org/abs/2207.10340).
- [2] B. Aubert *et al.* (BABAR Collaboration), The  $e^+e^- \rightarrow 2(\pi^+\pi^-)\pi^0, 2(\pi^+\pi^-)\eta, K^+K^-\pi^+\pi^-\pi^0$  and  $K^+K^-\pi^+\pi^-\eta$  cross sections measured with initial-state radiation, *Phys. Rev. D* **76**, 092005 (2007); **77**, 119902 (2008).
- [3] P. A. Zyla *et al.* (Particle Data Group), Review of particle physics, *Prog. Theor. Exp. Phys.* **2020**, 083C01 (2020).
- [4] A. Hasan and D. V. Bugg, Amplitudes for  $\bar{p}p \rightarrow \pi\pi$  from 0.36 GeV/c to 2.5 GeV/c, *Phys. Lett. B* **334**, 215 (1994).
- [5] D. V. Bugg, Four sorts of meson, *Phys. Rep.* **397**, 257 (2004).
- [6] M. Ablikim *et al.* (BESIII Collaboration), Observation of a resonant structure in  $e^+e^- \rightarrow \omega\eta$  and another in  $e^+e^- \rightarrow \omega\pi^0$  at center-of-mass energies between 2.00 and 3.08 GeV, *Phys. Lett. B* **813**, 136059 (2021).
- [7] M. Ablikim *et al.* (BESIII Collaboration), Measurement of the Born cross sections for  $e^+e^- \rightarrow \eta'\pi^+\pi^-$  at center-of-mass energies between 2.00 and 3.08 GeV, *Phys. Rev. D* **103**, 072007 (2021).
- [8] S. Godfrey and N. Isgur, Mesons in a relativized quark model with chromodynamics, *Phys. Rev. D* **32**, 189 (1985).
- [9] T. Barnes, F. E. Close, P. R. Page, and E. S. Swanson, Higher quarkonia, *Phys. Rev. D* **55**, 4157 (1997).
- [10] D. Ebert, R. N. Faustov, and V. O. Galkin, Mass spectra and Regge trajectories of light mesons in the relativistic quark model, *Phys. Rev. D* **79**, 114029 (2009).
- [11] Z. Y. Li, D. M. Li, E. Wang, W. C. Yan, and Q. T. Song, Assignments of the Y(2040),  $\rho(1900)$ , and  $\rho(2150)$  in the quark model, *Phys. Rev. D* **104**, 034013 (2021).
- [12] J. Z. Wang, L. M. Wang, X. Liu, and T. Matsuki, Deciphering the light vector meson contribution to the cross sections of  $e^+e^-$  annihilations into the open-strange channels through a combined analysis, *Phys. Rev. D* **104**, 054045 (2021).
- [13] L. M. Wang, S. Q. Luo, and X. Liu, Light unflavored vector meson spectroscopy around the mass range of 2.4–3 GeV and possible experimental evidence, *Phys. Rev. D* **105**, 034011 (2022).
- [14] L. P. He, X. Wang, and X. Liu, Towards two-body strong decay behavior of higher  $\rho$  and  $\rho_3$  mesons, *Phys. Rev. D* **88**, 034008 (2013).
- [15] J. C. Feng, X. W. Kang, Q. F. Lü, and F. S. Zhang, Possible assignment of excited light S31 vector mesons, *Phys. Rev. D* **104**, 054027 (2021).
- [16] T. Hilger, M. Gomez-Rocha, and A. Krassnigg, Light-quarkonium spectra and orbital-angular-momentum decomposition in a Bethe–Salpeter-equation approach, *Eur. Phys. J. C* **77**, 625 (2017).
- [17] T. Branz, T. Gutsche, V. E. Lyubovitskij, I. Schmidt, and A. Vega, Light and heavy mesons in a soft-wall holographic approach, *Phys. Rev. D* **82**, 074022 (2010).
- [18] G. L. Yu, Z. G. Wang, X. W. Wang, and H. J. Wang, The ground states and the first radially excited states of D-wave vector  $\rho$  and  $\phi$  mesons, *Int. J. Mod. Phys. A* **36**, 2150197 (2021).
- [19] L. Rosenberg, Electromagnetic interactions of neutrinos, *Phys. Rev.* **129**, 2786 (1963).
- [20] N. I. Kochelev, D. P. Min, Y. s. Oh, V. Vento, and A. V. Vinnikov, A new anomalous trajectory in Regge theory, *Phys. Rev. D* **61**, 094008 (2000).
- [21] O. Kaymakcalan, S. Rajeev, and J. Schechter, Nonabelian anomaly and vector meson decays, *Phys. Rev. D* **30**, 594 (1984).
- [22] T. Bauer and D. R. Yennie, Corrections to VDM in the photoproduction of vector mesons. I. Mass dependence of amplitudes, *Phys. Lett.* **60B**, 165 (1976).
- [23] T. Bauer and D. R. Yennie, Corrections to diagonal VDM in the photoproduction of vector mesons. II.  $\phi$ - $\omega$  mixing, *Phys. Lett.* **60B**, 169 (1976).
- [24] L. M. Wang, J. Z. Wang, and X. Liu, Toward  $e^+e^- \rightarrow \pi^+\pi^-$  annihilation inspired by higher  $\rho$  mesonic states around 2.2 GeV, *Phys. Rev. D* **102**, 034037 (2020).
- [25] Q. S. Zhou, J. Z. Wang, X. Liu, and T. Matsuki, Identifying the contribution of higher  $\rho$  mesons around 2 GeV in the  $e^+e^- \rightarrow \omega\pi^0$  and  $e^+e^- \rightarrow \rho\eta'$  processes, *Phys. Rev. D* **105**, 074035 (2022).